Continuous nematic anchoring transition due to surface-induced smectic order

Tatsutoshi Shioda, Bing Wen, and Charles Rosenblatt
Department of Physics, Case Western Reserve University, Cleveland, Ohio 44106-7079
(Received 22 November 2002; published 17 April 2003)

A continuous transition from tilted to homeotropic alignment at an interface is observed at a temperature T_a for a nematic liquid crystal on cooling toward the nematic–smectic-*A* phase transition temperature. T_a is found to depend on the treatment of the substrate. The behavior is examined theoretically in terms of a pair of competing easy axes (homeotropic and planar) and the tilt elasticity associated with the growth of surface-induced smectic order.

DOI: 10.1103/PhysRevE.67.041706 PACS number(s): 61.30.Gd

When a liquid crystal forms an interface with another material, the director at the interface $\hat{n}_i$ adopts an orientation that is determined by a combination of the interfacial properties, applied external fields, and torques due to elastic deformations in the bulk. There are two special orientations of $\hat{n}_i$: homeotropic orientation in which $\hat{n}_i$ is normal to the interface with polar "pretilt" angle $\theta_i = 0$, and planar orientation in which $\hat{n}_i$ lies in the plane of the interface with $\theta_i = \pi/2$. For planar orientation, the azimuthal angle φ may be controlled by manipulation of the surface—for example, one may rub unidirectionally a polyimide-coated substrate—or φ may be 2π-fold degenerate. In 1981, Känel *et al.* showed that a discontinuous transition from planar to homeotropic orientation occurs at a flat glass or quartz substrate on cooling toward the smectic-*A* phase transition temperature T_{NA} [1]. Ascribing this result to the onset of surface-induced smectic order in the nematic phase, they also showed that sufficiently deep ion-etched gratings tend to suppress this transition. In general, however, the pretilt angle θ_i need not be 0 or $\pi/2$, but may adopt any value in between. In 1983, Chiarelli *et al.* demonstrated a continuous anchoring transition at the free surface of a nematic liquid crystal [2,3], whereby θ_i was found to be zero above an anchoring transition temperature T_i; below T_i they found a mean field exponent $\beta = 0.5 \pm 0.04$ for θ_i vs reduced temperature. DiLisi *et al.* measured the polar anchoring strength coefficient A for a homeotropically-oriented dimeric liquid crystal at a phospholipid-coated substrate [4], where A is defined by the lowest-order contribution to the interfacial term of the free energy, viz., $F_i = \frac{1}{2} A \sin^2(\theta_i - \theta_p)$. F_i represents the energy cost of a director orientation θ_i that differs from the polar angle θ_p of the preferred axis; this deviation may be due to an externally applied field or to an elastic torque. [Note that this form for the free energy preserves the symmetry $F_i(\theta_i) = F_i(\theta_i + \pi)$.] DiLisi *et al.* found that A first increases, then decreases with decreasing temperature in the nematic phase, eventually vanishing at an anchoring transition temperature T_i; for $T < T_i$ the polar angle θ_p of the preferred axis becomes nonzero, and therefore so does the actual director angle θ_i in the absence of an external field or elastic torque. Subsequently, many other interfacial transitions have been observed. Temperature has been shown to be an important parameter in causing interfacial transitions [5]. Some transitions have been generated by *in situ* chemical changes to the surface [6,7], such as ultraviolet light exposure of the surface coating [8,9], changes in the hydrophobicity of the substrate [10], or the length and surface coverage of a surfactant molecule [11]. In other cases, substrate-adsorbed ions or other impurities have been shown to induce an anchoring transition [12–14]. In this paper, we report on an anchoring transition driven by the approach of the smectic-*A* phase. Although the mechanism that drives homeotropic order is similar to that reported in Ref. [1], our transition involves a *continuous* change of θ_i rather than a discontinuous switching between two extreme states, planar and homeotropic [1].

In a recent paper we showed that judicious processing of a polyimide can facilitate exquisite control over θ_i [15], where θ_i can be varied from 0 to as high as $\sim \pi/4$ in the nematic phase, depending upon the liquid crystal. On approaching the nematic–smectic-*A* phase transition temperature T_{NA} from above, however, the presence of a smooth interface tends to induce smectic layering at the interface [16–18]. The smectic order decays from the substrate into the bulk on a length scale of the order of the temperature-dependent smectic correlation length ξ [1,17], although the order can be disrupted by surface roughness [19]. Due to the surface-induced smectic order there exists an elastic constant D ($\propto \langle \psi^2 \rangle$ where ψ is the induced smectic order parameter) that attempts to keep the molecules oriented normal to the smectic layer [20]. This has the effect of enhancing the effective anchoring strength coefficient for homeotropic alignment and driving θ_i toward zero. Our central result is the observation of a continuous anchoring transition at temperature T_a on cooling the liquid crystal toward T_{NA}, below which $\theta_i = 0$. The quantity $\Delta T \equiv T_a - T_{NA}$ is found to be small for cells having a large pretilt angle and large for small pretilt angle cells. A Landau model for the phenomenon is presented.

Hybrid cells were constructed by using microscope glass cleaned in detergent, acetone, and ethanol, and then spin coated with the polyimide SE1211 (Nissan Chemicals). Under ordinary cirumstances, the polyimide baking regimen specified by the manufacturer promotes homeotropic liquid crystal alignment. However, we have found that a longer baking time followed by unidirectional rubbing of the polyimide promotes a large pretilt angle θ_i [15]. We suggested that the extra baking enhances the degree of imidization of the polymer, and that the unidirectional rubbing extends the now more rigid backbone. $\hat{n}_i$ then adopts an equilibrium

angle θ_i that is determined by the relative interactions of the molecules with the planar-promoting backbone and the homeotropic-promoting side chains. For the present experiment we baked the polyimide-coated glass at 180 °C for 1 h. One glass slide (surface ''1'') was left unrubbed to promote homeotropic alignment. Four squares, each measuring 50 μm$\times$50 μm and containing 300 parallel lines (spaced 167-nm apart), were scribed on the other slide (surface ''2'') by a 20-nm-diameter silicon stylus of an atomic force microscope (AFM). By using an AFM as opposed to a cotton cloth, we were able to create a region of very uniform rubbing and therefore a spatially uniform interaction potential with the liquid crystal. The forces used for successive squares were 1.2, 1.9, 2.7, and 4.1 μN. By using the AFM in noncontact mode, the resulting grooves in the polyimide coating were found to have peak-to-peak distances of 6.2, 9.2, 17, and 24 nm. The two slides were placed together, separated by Mylar spacers, and cemented at the edges. The thickness d of the empty cell was determined by means of a spectrometer, whose spectrum ranged from 400 nm through 800 nm. By measuring the wavelengths λ of consecutive maxima m and $m+1$, the thickness $d=17.1\pm0.9$ μm was determined from the formula $d=(\lambda_{m+1}^{-1}-\lambda_m^{-1})^{-1}/2$. The cell then was filled in the isotropic phase with the liquid crystal SCE12R (Merck) and cooled into the nematic phase. [Having examined several liquid crystalline materials, we found that the polar tilt angle θ_i for a given surface preparation varies greatly from one liquid crystal to another. Since (a) it has a large pretilt in the nematic phase, (b) it remains liquid crystalline at room temperature, and (c) has a large body of available material data, we chose to study the racemic mixture SCE12R.]

Optical retardation measurements were performed in order to determine the polar tilt angle θ_i at the AFM-scribed substrate. Light from a He-Ne laser passed consecutively through a polarizer, the sample (oriented such that the director's azimuthal orientation made a 45 ° angle with respect to the polarizer), a Pockels cell modulated at frequency $\nu=318$ Hz, an $f=5$ mm focal length lens, a mask, an analyzer, and into a detector. The lens was placed slightly more than one focal length from the sample, thereby creating an image of the sample that was enlarged by a factor of 30 at the mask. The mask was then centered over the image of the AFM-scribed square, allowing the detector to sample light that passes only through the square. The output from the detector was fed into a lock-in amplified referenced to frequency ν, and the lock-in output was integrated over time. The integrated voltage was used to control a dc power supply such that it supplied a voltage to the Pockels cell sufficient to cancel the optical retardation α of the cell. The voltage applied to the automatically compensated Pockels cell therefore was proportional to α. By measuring the Pockels cell voltage, the optical retardation was determined continuously as the temperature was decreased at a rate of ≈0.01 K s^{-1}. The retardation α for all four squares is shown in Fig. 1.

In order to convert the retardation data into polar tilt angles θ_i at the interface, we first measured the ordinary and extraordinary refractive indices n_o and n_e, respectively, with an Abbe refractometer illuminated with light from a He-Ne laser at wavelength $\lambda=632.8$ nm. Over the temperature range of interest, which is more than 30 K below the nematic-isotropic transition temperature $T_{NI}=118$ °C, the refractive indices were nearly constant. Therefore, throughout our analysis we used the values $n_o=1.481$ and $n_e=1.638$. The retardation $\alpha=\int_{z=0}^{d}[2\pi\Delta n(\theta)/\lambda]dz$, where the effective birefringence $\Delta n(\theta)=n_o n_e(n_o^2\sin^2\theta+n_e^2\cos^2\theta)^{-1/2}-n_o$. Our task now is to determine the profile of the polar angle $\theta(z)$ in bulk as a function of position z in the cell. The extrapolation length L for an elastic distortion is given by $L=K/A$, where K is an appropriate elastic constant. For an AFM-scribed substrate and deep into the nematic phase, A is of the order of 1×10^{-1} erg cm^{-2} [21,22]. Because surface 1 was treated for homeotropic alignment ($\theta_{i=1}\approx0$) and, as we shall see below, the polar angles $\theta_{i=2}$ at surface 2 are generally less than 20 °, the relevant elastic constant is primarily bend, K_{33}. The bend elastic constant diverges near T_{NA}, although in the temperature region of interest for SCE12R K_{33} takes on values between 1 and 4 $\times10^{-6}$ dyn [15]. Thus, $0.1<L<0.4$ μm over the temperature region that was investigated. Since L is considerably smaller than d, the two surfaces are approximately uncoupled and therefore we may take $\theta_1\approx0$. [Note that even if θ_1 were nonzero, it would make a very small contribution to the retardation because $\Delta n(\theta_1)$ would be very small.] Because the elastic distortion is nearly pure bend, the Euler equation $K_{33}(d^2\theta/dz^2)=0$ derived from the elastic free energy [20] yields a solution $\theta=\theta_2(z/d)$. [If we were to include the splay elastic constant $K_{11}=1\times10^{-6}$ dyn, our numerical simulations show that the maximum deviation from the form $\theta(z)$ is at most 2%.] θ_2 is determined by matching the calculated value of the retardation α with the measured value in Fig. 1. Figure 2 shows the deduced values of the polar tilt angle θ_2 at the AFM-scribed substrate, using the approximation that the two surfaces are noninteracting. To make certain that the anchoring transition is continuous, we have exam-

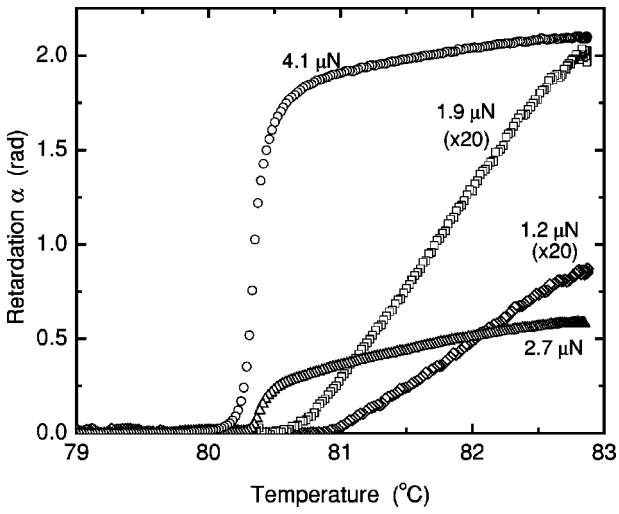

FIG. 1. Retardation vs temperature for four different rubbing forces. Note that for presentation purposes the data for the two smallest forces, viz., 1.2 and 1.9 μN, have been multiplied by a factor of 20.

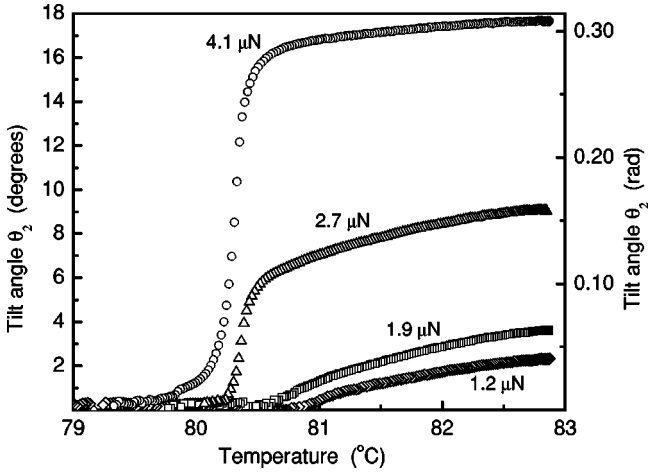

FIG. 2. Derived tilt angle θ_2 (in degrees at left and radians at right) vs temperature for four different forces. Unlike Fig. (1), none of the data sets in this figure has been scaled by a factor of 20.

ined the possibility of hysteresis by ramping temperature both down *and* up at a rate of 0.0005 K s^{-1}. Figure 3 shows a typical trace. As no hysteresis was observed, we believe that the transition is continuous. The main points of this work are that the transition is continuous and the transition temperature depends on the rubbing strength. As an aside, we point out that although it would have been easier to scribe *both* surfaces and arrange them antiparallel to each other in order that $\theta_1=\theta_2$, with no elastic distortion in the cell, we have chosen to use a hybrid cell because of the difficulty in getting the 50 μm$\times$50 μm squares at the two substrates into register.

As is clear from both Figs. 1 and 2, an anchoring transition occurs at a temperature T_a close to T_{NA}. Moreover, the anchoring transition occurs closer to T_{NA} for regions that are more strongly rubbed and that exhibit a larger pretilt angle θ_2 in the nematic phase. In order to understand this behavior,

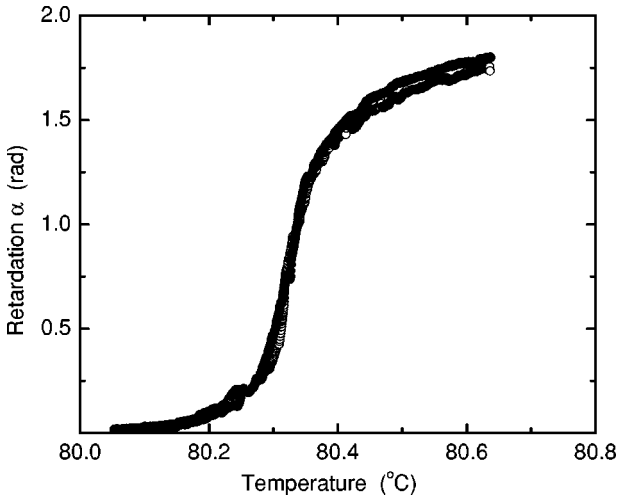

FIG. 3. Retardation vs temperature for 4.1-μN square. Open circles correspond to the heating curve and solid circles to the cooling curve. Heating and cooling rates were 0.0005 K s^{-1}. No apparent hysteresis is observed.

we propose a model in which the unrubbed polyimide promotes homeotropic alignment with an anchoring strength coefficient A_i, where $i=1,2$. Rubbing of the polyimide induces alignment of the backbone, which we conjecture creates a second easy axis (for planar alignment) on surface 2 with anchoring strength B_2. The rubbing also implies that A_1 may not be equal to A_2. Since the two easy axes (homeotropic and planar) on surface 2 compete, we need to introduce a higher-order term in the interfacial free energy, $C_2 \sin^4\theta_2$, to determine the equilibrium polar angle θ_2 of the director $\hat{n}_i$. The coefficient C_2, which may depend upon the rubbing strength, must be positive on an empirical basis because θ_2 is found to be relatively small above the anchoring transition temperature T_a. Additionally, we assume that surface-induced smectic layers grow at the substrates over a distance ξ into the bulk, where ξ is the temperature-dependent correlation length [1,17,19]. This introduces an additional temperature-dependent elastic constant D into the problem, whose role is to maintain the director orientation parallel to the layer normal. The total free energy per unit area F is given by

$$F=\frac{1}{2}\left[\int_0^d dz\left\{(K_{11}\sin^2\theta+K_{33}\cos^2\theta)\left(\frac{\partial\theta}{\partial z}\right)^2+D(e^{(z-d)/\xi}+e^{-z/\xi})\sin^2\theta\right\}+A_2\sin^2\theta_2+B_2\cos^2\theta_2+C_2\sin^4\theta_2+A_1\sin^2\theta_1\right], \quad (1)$$

where $z=0$ at surface 1 and $z=d$ at surface 2. Although the large number of parameters precludes a detailed data fit, we shall discuss the qualitative behavior of Eq. (1). Because $L\ll d$ and $\theta<20°$, for now we shall neglect the term $K_{11}\sin^2\theta(\partial\theta/\partial z)^2$ and take $K_{33}\cos^2\theta(\partial\theta/\partial z)^2 \approx K_{33}(\partial\theta/\partial z)^2$. Moreover, we shall neglect the terms $De^{-z/\xi}\sin^2\theta$ and $A_1\sin^2\theta_1$ near the (almost) homeotropic surface 1; these restrictions will be relaxed later. Additionally, because ξ is at most 100 nm, the term $De^{(z-d)/\xi}\sin^2\theta$ is non-negligible only in a thin surface layer, where we can approximate θ as a constant equal to θ_2. With these approximations the integral becomes $\int_0^d dz\,\frac{1}{2}[K_{33}(\partial\theta/\partial z)^2+De^{(z-d)/\xi}\sin^2\theta]\approx(1/2d)K_{33}\theta_2^2+\frac{1}{2}D\xi\sin^2\theta_2$, where we have assumed that $\theta_1=0$. The free energy becomes

$$F\approx\frac{1}{2}\left[\frac{1}{d}K_{33}\theta_2^2+B_2+(D\xi+A_2-B_2)\sin^2\theta_2+C_2\sin^4\theta_2\right]. \quad (2)$$

Let us first consider the behavior in the absence of surface-induced smectic order ($D=0$) in the limit of a very thick cell (large d). We minimize F with respect to $\sin\theta_2$ and find that $\sin\theta_2=\sqrt{(B_2-A_2)/2C_2}$ for $B_2>A_2$ and $\sin\theta_2=0$ for $B_2<A_2$. It is important to stress that this is qualitatively the behavior observed in measurements of pretilt angle of the liquid crystal pentylcyanobiphenyl at a rubbed SE1211-coated substrate [15]: Below a critical rubbing

strength the pretilt angle is zero, and it rises continuously with approximately this form above the critical rubbing strength. *In other words, there is a minimum rubbing strength required before the pretilt angle becomes nonzero.* For rubbing strengths weaker than those reported herein, we found that θ_2 remains zero even well above T_{NA}, presumably because B_2 is small. The addition of surface-induced smectic order ($D \neq 0$) has the consequence of increasing the *effective* (quadratic) anchoring strength coefficient for homeotropic order; the same holds true for the elastic term, which exerts a (small) torque at surface 2. As T_{NA} is approached from above the term $D\xi$ grows algebraically, the coefficient of the $\sin^2\theta_2$ term in Eq. (2) becomes positive, and there is a transition to homeotropic alignment at temperature T_a. Moreover, because B_2 increases with increasing rubbing strength (cf. Ref. [15]), the temperature T_a at which the transition occurs decreases with increasing rubbing strength, as is evident in Figs. 1 and 2. Consistent with Eq. (2), we note that no such anchoring transition to homeotropic order was observed for the liquid crystal pentylcyanobiphenyl [15] due to the absence of a smectic-*A* phase in that material.

Let us now return to Eq. (2). We can examine the behavior close to T_a where θ_2 is small and expand F for small values of θ_1 and θ_2. Thus $\sin\theta_2 \sim \theta_2$. Moreover, we shall partially relax the restrictions on θ_1: We shall now include the terms $A_1 \sin^2\theta_1 \sim A_1\theta_1^2$ and $D\xi \sin^2\theta_1 \sim D\xi\theta_1^2$, and approximate $(d\theta/dz)^2$ as $[(\theta_1-\theta_2)/d]^2$. Minimizing F with respect to θ_1, we find $\partial F/\partial\theta_1 = (1/d)K_{33}(\theta_1-\theta_2)+(A_1+D\xi)\theta_1 = 0$, and therefore

$$\theta_1 = \frac{K_{33}}{K_{33}+(A_1+D\xi)d}\,\theta_2. \tag{3}$$

On substituting θ_1 into the free energy, we obtain

$$\begin{aligned} F &= \frac{1}{2}\left[\frac{1}{d}K_{33}\left(\frac{K_{33}}{K_{33}+(A_1+D\xi)d}-1\right)^2\theta_2^2+(D\xi+A_2-B_2)\,\theta_2^2\right. \\ &\quad \left. + C_2\theta_2^4 + A_1\left(\frac{K_{33}}{K_{33}+(A_1+D\xi)d}\right)^2\theta_2^2\right] \\ &= \frac{1}{2}(\gamma\theta_2^2+C_2\theta_2^4), \end{aligned} \tag{4}$$

where

$$\begin{aligned} \gamma &= \frac{1}{d}K_{33}\left(\frac{K_{33}}{K_{33}+(A_1+D\xi)d}-1\right)^2+(D\xi+A_2-B_2) \\ &\quad + A_1\left(\frac{K_{33}}{K_{33}+(A_1+D\xi)d}\right)^2. \end{aligned} \tag{5}$$

Equation (4) has only one solution, $\theta_2 = 0$, for $\gamma, C_2 > 0$; this occurs when the rubbing is weak and B_2 is small. Another solution $\theta_2^2 = -\gamma/2C_2$ exists for $\gamma < 0$; this solution has lower energy ($F = -\gamma^2/4C_2$) than the $\theta_2 = 0$ solution, for which $F = 0$. The transition from one regime to the other is second order. Experimentally, this predicted behavior is observed unambiguously for the two weaker rubbing strengths, viz., 1.2 and 1.9 μN, where the retardation α (which is approximately proportional to θ_2^2) varies linearly with temperature even well above T_a; this is seen in Fig. 1. For stronger rubbing strengths, the predicted behavior is less obvious. We note that for stronger rubbing the quantity B_2 becomes large, requiring a large value of $D\xi$ before a transition to $\theta_2 = 0$ can occur. Since the quantity $D\xi$ varies very rapidly close to T_{NA}, an expansion of γ in powers of temperature would require the incorporation of higher-order terms, even moderately close to T_a. Thus, one would expect a rapid linear increase of the retardation only very close to T_a, followed by a shoulder and a much less rapid rise at higher temperatures; indeed, this is the behavior observed in Fig. 1. We note that the small amount of rounding observed near T_a in the strong rubbing strength data, especially for a force of 4.1 μN, likely is due to small inhomogeneities in the square. Again, the rapid variation of $D\xi$ in this region causes rounding very close to T_a. Finally, as noted above, no hysteresis was observed on cooling and heating (cf. Fig. 3), further evidence of a continuous transition.

We can estimate the importance of the various contributions to γ in Eq. (5). We assume that $A_1 \sim A_2 \sim B_2 \sim 10^{-1}$ erg cm^{-2} deep inside the nematic phase [22], $K_{33} \sim 4\times10^{-6}$ dyn at $T = T_{NA}+1$ K [15], and $d \sim 10^{-3}$ cm. The situation is more complicated for D and ξ. Taking $D = D_0\langle\psi^2\rangle$, Sinha *et al.* found $D_0 = (3.5\pm0.9)\times10^7$ erg cm^{-3} [19]. For a typical flat interface Mirantsev calculated a surface-induced smectic order parameter $\psi \sim 0.5$, ≈ 30 mK above T_{NA}. Since $\langle\psi^2\rangle \propto [(T-T_{NA})/T_{NA}]^{-2\nu}$, where ν is the correlation length critical exponent, at $T = T_{NA}+1$ K we would find a value $\langle\psi^2\rangle \sim 0.0005$ for $\nu = 0.9$ [19] or $\langle\psi^2\rangle \sim 0.002$ if ν had the more typical value 0.7 [23]. These would correspond to $D \sim 1.6\times10^4$ and 6.5×10^4 erg cm^{-3}, respectively. Using a bare correlation length $\xi_0 = 5.3\times10^{-8}$ cm [19], at $T = T_{NA}+1$ K we find correlation lengths of $\xi = 9\times10^{-6}$ cm and $\xi = 3\times10^{-6}$ cm for $\nu = 0.9$ and 0.7, respectively. Thus, $D\xi \sim 0.1$–0.2 erg cm^{-2} for both exponents ν. Such values for $D\xi$ are of the same order as the quadratic anchoring coefficients, indicating that the anchoring transition temperature T_a would be of the order of a few hundred millikelvins to a few degrees kelvin above T_{NA}, as observed experimentally. Thus, in Eq. (5) the orders of magnitude for the elastic energy, anchoring energy at the scribed surface, and anchoring energy at the unscribed surface, respectively, are 10^{-3}, 10^{-1}, and 10^{-5} erg cm^{-2}. Clearly the anchoring term dominates, and our experimental use of a hybrid cell and assumption that the two surfaces are largely noninteracting are valid.

As noted originally by Känel *et al.* [1], surface-induced smectic order in the nematic phase can drive an anchoring transition to homeotropic orientation. We have demonstrated here that such a transition may be continuous with a transition temperature T_a that depends on the rubbing strength. Moreover, we have shown experimentally that such a transition may be limited to a very narrow range of surface treatment conditions. From a theoretical standpoint, we suggested that rubbing gives rise to a pair of easy axes. Multiple easy axes, which have been observed previously by optical con-

trol of the surface [24,25], may be used to explain our earlier results [15], wherein there exists a nonzero threshold rubbing strength below which the director remains homeotropic. Coupled with surface-induced smectic order, the model qualitatively explains our current results, viz., there exists only a narrow range of rubbing strengths that facilitates observation of an anchoring transition, and there is an inverse relationship between T_a and the rubbing strength.

This work was supported by the U.S. Department of Energy's Office of Basic Energy Science under Grant No. DE-FG02-01ER45934; by the U.S. Department of Energy's Nanoscale Science, Engineering, and Technology Program at Brookhaven National Laboratory under Contract No. DE-AC02-98CH10886 and by the Donors of the Petroleum Research Fund, administered by the American Chemical Society, under Grant No. 37736-AC7.

[1] H.V. Känel, J.D. Litster, J. Melngailis, and H.I. Smith, Phys. Rev. A **24**, 2713 (1981).
[2] P. Chiarelli, S. Faetti, and L. Fronzoni, J. Phys. (Paris) **44**, 1061 (1983).
[3] P. Chiarelli, S. Faetti, and L. Fronzoni, Phys. Lett. **101A**, 31 (1984).
[4] G.A. DiLisi, C. Rosenblatt, A.C. Griffin, and U. Hari, Liq. Cryst. **7**, 353 (1990).
[5] L. Komitov, P. Rundquist, A. Strigazzi, and M. Warenghem, Mol. Cryst. **282**, 259 (1996).
[6] G.P. Crawford, R.J. Ondris-Crawford, J.W. Doane, and S. Zumer, Phys. Rev. E **53**, 3647 (1996).
[7] K.R. Amundson and M. Srinivasarao, Phys. Rev. E **58**, R1211 (1998).
[8] L. Komitov, K. Ichimura, and A. Strigazzi, Liq. Cryst. **27**, 51 (2000).
[9] H. Akiyama and Y. Iimura, Jpn. J. Appl. Phys., Part 2 **40**, L765 (2001).
[10] B. Alkhairalla, H. Allinson, N. Boden, S.D. Evans, and J.R. Henderson, Phys. Rev. E **59**, 3033 (1999).
[11] T. Jin, G.P. Crawford, R.J. Crawford, S. Zumer, and D. Finotello, Phys. Rev. Lett. **90**, 015504 (2003).
[12] V.G. Nazarenko and O.D. Lavrentovich, Phys. Rev. E **49**, R990 (1994).
[13] V.G. Nazarenko, V.M. Pergamenshchik, O. Koval'chuk, and B.I. Lev, Mol. Cryst. Liq. Cryst. Sci. Technol., Sect. A **352**, 435 (2000).
[14] R. Barberi, M. Giocondo, M. Iovane, I. Dozov, and E. Polossat, Liq. Cryst. **25**, 23 (1998).
[15] G.P. Sinha, Bing Wen, and C. Rosenblatt, Appl. Phys. Lett. **79**, 2543 (2001).
[16] J. Als-Nielsen, F. Christensen, and P.S. Pershan, Phys. Rev. Lett. **48**, 1107 (1982).
[17] C. Rosenblatt, Phys. Rev. Lett. **53**, 791 (1984).
[18] B.M. Ocko, Phys. Rev. Lett. **64**, 2160 (1990).
[19] G.P. Sinha, C. Rosenblatt, and L.V. Mirantsev, Phys. Rev. E **65**, 041718 (2002).
[20] P.G. DeGennes and J. Prost, *Physics of Liquid Crystals* (Clarendon, Oxford, 1994).
[21] Bing Wen and C. Rosenblatt, J. Appl. Phys. **89**, 4747 (2001).
[22] C. Rosenblatt, J. Phys. (Paris) **45**, 1087 (1984).
[23] C.W. Garland and G. Nounesis, Phys. Rev. E **49**, 2964 (1994).
[24] D. Andrienko, Y. Kurioz, Y. Reznikov, and V. Reshetnyak, JETP **85**, 1119 (1997).
[25] D. Andrienko, Y. Kurioz, Y. Reznikov, C. Rosenblatt, R.G. Petschek, O.D. Lavrentovich, and D. Sebacius, J. Appl. Phys. **83**, 50 (1998).